Repository Istituzionale dei Prodotti della Ricerca del Politecnico di Bari

Multistability and localization in forced cyclic symmetric structures modelled by weakly-coupled Duffing oscillators

This is a pre-print of the following article

Original Citation:
Multistability and localization in forced cyclic symmetric structures modelled by weakly-coupled Duffing oscillators / Papangelo, A.; Fontanela, F.; Grolet, A.; Ciavarella, M.; Hoffmann, N.. - In: JOURNAL OF SOUND AND VIBRATION. - ISSN 0022-460X. - STAMPA. - 440:(2019), pp. 202-211. [10.1016/j.jsv.2018.10.028]

Availability:
This version is available at http://hdl.handle.net/11589/175770 since: 2022-06-08

Published version
DOI:10.1016/j.jsv.2018.10.028

Publisher:

Terms of use:

(Article begins on next page)

02 May 2026

Link to the publisher version
https://doi.org/10.1016/j.jsv.2018.10.028

Multistability and localization in forced cyclic symmetric structures modelled by weakly-coupled Duffing oscillators

A. Papangelo[(1,2,*)], F. Fontanela[(3)], A. Grolet[(4)], M. Ciavarella[(1,2)], N. Hoffmann[(2,3)]

[(1)] *Politecnico di BARI. DMMM dept. V Gentile 182, 70126 Bari, Italy*

[(2)] *Hamburg University of Technology, Department of Mechanical Engineering, Am Schwarzenberg-Campus 1, 21073 Hamburg, Germany*

[(3)] *Imperial College London, Exhibition Road, London SW7 2AZ , UK*

[(4)] *Arts et Métiers ParisTech, Department of Mechanical Engineering, 8 Boulevard Louis XIV, 59000 Lille, France*

[(*)] *email: antonio.papangelo@poliba.it*

Abstract

Many engineering structures are composed of weakly coupled sectors assembled in a cyclic and ideally symmetric configuration, which can be simplified as forced Duffing oscillators. In this paper, we study the emergence of localized states in the weakly nonlinear regime. We show that multiple spatially localized solutions may exist, and the resulting bifurcation diagram strongly resembles the snaking pattern observed in a variety of fields in physics, such as optics and fluid dynamics. Moreover, in the transition from the linear to the nonlinear behaviour isolated branches of solutions are identified. Localization is caused by the hardening effect introduced by the nonlinear stiffness, and occurs at large excitation levels. Contrary to the case of mistuning, the presented localization mechanism is triggered by the nonlinearities and arises in perfectly homogeneous systems.

Keywords: nonlinear vibrations, nonlinear normal modes, multistability, localization

1. Introduction

The aerospace and aeronautical industries face an increasing effort to improve machine performances [1]. Within this scenario, several new designs have been proposed, some of which relying on lightweight materials applied to e.g. bladed disks, satellites, and space antennas. The resulting slender structures may undergo large deflections and nonlinear phenomena such as energy localization may be observed.

The problem of energy localization is a well-known phenomenon within the vibration engineering community, particularly in turbomachinery [2, 3], aerospace structures [4] but also in microelectromechanical systems [5, 6]. In the linear framework, indeed, that community usually refers to the behaviour as a mistuning problem due to its relevance for the design of bladed disks [2, 7]. In this case, localization arises due to the break of symmetry induced by inhomogeneities from manufacturing variability or wear. From the modelling perspective, the capability of computing the level of localization has been extensively addressed [8, 9], although a real solution to the problem has not been found: small changes of the mass distribution (due to erosion or wear) during service make any clever solution impossible, and design has to take into account worst case scenarios involving significant amplification of vibration with respect to the homogeneous case. Linear energy localization is known also more in general in other research fields. For example, in the solid state physics community, it is known as "Anderson localization", as the phenomenon was firstly studied by Anderson [10] in the context of a diffusion wave problem, and was a Nobel-prize discovery. Nevertheless, in complex engineering applications the linear behaviour has to be seen as an approximation, as non-linearities emerge in either stiffness or damping elements. In the case of energy dissipation in bladed disks, for example, vibration control usually relies on passive components, such as frictional dampers and this induces both non-linearities due to the contact status and to the frictional law [11–16]. Therefore, even the standard vibration control technique implemented in the aerospace industry inherently introduces nonlinearity to the physical systems.

For aeronautical applications the so-called "blisk" have been developed, where contact surfaces between the disk and the blade root are avoided as the whole structure is built monolithically. Due to the lack of frictional dissipation in joints, blisks suffer the lack of sufficient damping, which can expose the structures to large deformation regimes, where geometric nonlinearities

have an important role. In this case, energy localization goes much beyond mistuning (see e.g. [17, 18]). It is well-known, for example, that even perfect cyclic and symmetric structures may localize energy, due to the evolution of non-similar modes or due to bifurcations, i.e. qualitative changes in system dynamics (see e.g. [19–28]). Nonlinear localization has been shown to appear not only in conservative systems [19] but also in friction-excited chains of weakly coupled oscillators [20, 21], where the authors showed that the localization phenomenon is strongly related to the bistable behaviour of the single oscillator in the chain. In the bifurcation diagram snaking-like bifurcations appear that strongly resemble the "snaking bifurcations" observed in different physics fields, such as fluid dynamics [29–31] and nonlinear optics [29].

In this paper, we study an harmonically forced cyclic and symmetric system made of a chain of Duffing oscillators with weak nearest-neighbour elastic coupling. The system can be seen as a minimal model for several cyclic and symmetric structures in the weakly nonlinear regime. It will be shown that the level of vibration localization depends on the forcing level, and it disappears in the case of low excitation when the system tends to the linear behaviour. Moreover, in the transition from low to high excitation, isolas of solutions appear. When the forced response is compared with the nonlinear normal modes of the system, it is shown that local resonances perfectly overlap with a particular backbone curve.

Notice that the mechanical system under study is homogeneous in space, thus the localization phenomenon occurs due to the inherent nonlinearities in the system (cubic stiffness terms) and is not related to any kind of inhomogeneity. In the last part of the paper we discuss the results obtained and point to possible further extension of this work.

2. A lumped nonlinear model for cyclic symmetric structures

The model under study consists of N_s identical oscillators with mass m, cyclically connected to each other by linear springs k_c, and also attached to the ground by linear springs and viscous dampers k_l and c, respectively (Fig. 1). Each oscillator is also excited by an external force $f_n(t)$ and is subjected to nonlinear forces induced by the cubic stiffness k_{nl}. The physical system in Fig. 1 can be considered a minimal model for aerospace structures, e.g. blisks, antennas, or reflectors, undergoing large deformations.

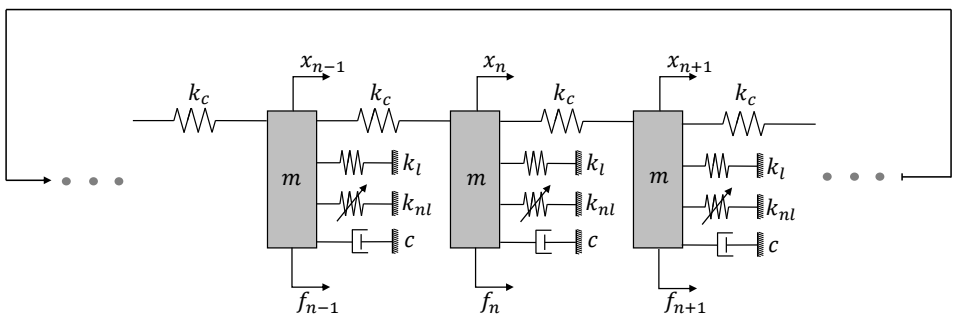

Fig. 1 - Minimal model for a cyclic and symmetric structure undergoing large displacements

The equation of motion for the n-th oscillator is written as

$$m\ddot{x}_n + c\dot{x}_n + k_l x_n - k_c(x_{n+1} + x_{n-1} - 2x_n) + k_{nl}x_n^3 = f_n(t) \tag{1}$$

where $\ddot{x}_n$, $\dot{x}_n$, and x_n are the acceleration, velocity, and displacement, respectively, while $f_n(t)$ represents the corresponding external force applied to the n-th mass. Equation (1) is rewritten, for convenience, such that

$$\ddot{x}_n + 2\xi\omega_0\dot{x}_n + \omega_0^2 x_n - \omega_c^2(x_{n+1} + x_{n-1} - 2x_n) + \gamma x_n^3 = \frac{f_n(t)}{m}, \tag{2}$$

where $\omega_0^2{=}\frac{k_l}{m}$, $\omega_c^2{=}\frac{k_c}{m}$, $\gamma{=}\frac{k_{nl}}{m}$, and $\xi{=}\frac{c}{2\sqrt{mk_l}}$. Finally, the set of nonlinear differential equations is expressed in non-dimensional form as

$$\ddot{u}_n + 2\xi\dot{u}_n + u_n - \alpha(u_{n+1} + u_{n-1} - 2u_n) + u_n^3 = g_n(\tau), \tag{3}$$

where the dots represent the derivative with respect to the new time scale $\tau = \omega_0 t$, $\alpha = \frac{\omega_c^2}{\omega_0^2}$, $A = \frac{\omega_0}{\sqrt{\gamma}}$, $g_n(\tau) = \frac{f_n(t)}{k_l A}$, and $x_n(t){=}Au(\tau)$. Moreover, one has the cyclic boundary condition $u_{N_s+1} = u_1$ and $u_0 = u_n$.

3. Conservative regime: linear analysis

The linear and conservative regime of Eq. (3), for which the equation of motion is given by:

$$\ddot{u}_n + u_n - \alpha(u_{n+1} + u_{n-1} - 2u_n) = 0, \tag{4}$$

has been previously studied in the literature (see e.g. Refs. [22]). The system has analytical travelling wave solutions such that

$$u_n(\tau) = U_n^k \exp\{\mathrm{i}\,[k(n-1)a - \omega_k \tau]\} + \text{c.c}, \tag{5}$$

where U^k is the complex wave amplitude, $a = 2\pi/N_s$ is the sector angle, k is the wave number, ω_k is the natural angular frequency, while c.c. states the complex-conjugate of the first expression. After inserting Eq. (5) into Eq. (4), it is possible to demonstrate that the linear dispersion relation is given by

$$\omega_k^2 = 1 + 2\alpha\,[1 - \cos(ka)]\,, \tag{6}$$

which represents the natural angular frequencies of Eq. (4). Moreover, the corresponding eigenvectors are obtained by substituting Eq. (6) into Eq. (5), and three different solutions are possible: (1) if $k = 0$ all masses move in phase such as $U_n^{k=0} = 1$; (2) if N_s is even $k \in [1, \frac{N_s}{2} - 1]$ (if N_s is odd $k \in [1, \frac{(N_s-1)}{2} - 1]$) two sets of solutions are possible such as $U_n^{k,cos}$=$\cos((n-1)ka)$ and $U_n^{k,sin}$=$\sin((n-1)ka)$; while (3) if $k = \frac{N_s}{2}$ the masses move out of phase such as $U_n^{k=\frac{n}{2}}$=$(-1)^n$. In Fig. 2 the linear mode shapes are shown assuming $N_s = 6$. Notice that the mode shapes (eigenvectors) do not depend on the coupling parameter α.

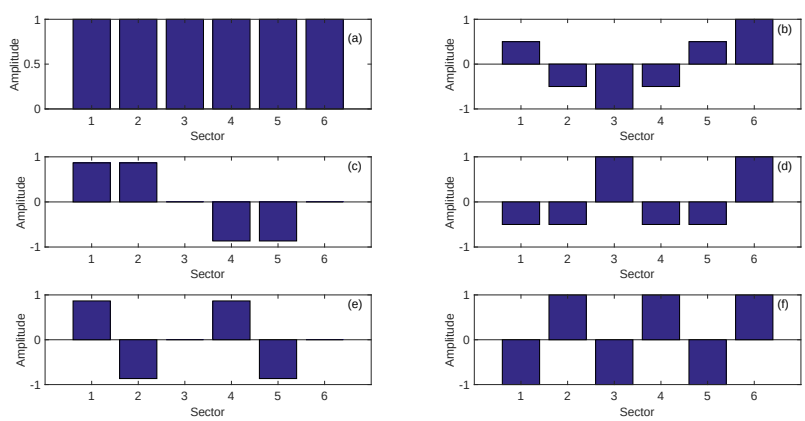

Fig. 2 - Linear mode shapes of the system with $N_s = 6$.

4. Nonlinear normal modes

4.1. General analysis

In the nonlinear and conservative regime our investigation is based on the concept of nonlinear modes ([32],[33]). Therefore, periodic vibrations in the form of

$$\ddot{u}_n + u_n - \alpha(u_{n+1} + u_{n-1} - 2u_n) + u_n^3 = 0 \tag{7}$$

are computed using only one harmonic such as

$$u_n = U_n \exp\{\omega\tau\} + c.c., \tag{8}$$

where U_n is the complex-valued amplitude and ω is the nonlinear natural angular frequency. The previous expression (8) is inserted into Eq. (7) and the resulting equation is projected into the Fourier basis which, neglecting higher order harmonics, leads to the following set of algebraic equations

$$(1 + 2\alpha - \omega^2)U_n + 3U_n^3 - \alpha(U_{n+1} + U_{n-1}) = 0. \tag{9}$$

The solutions of Eq. (9) define the nonlinear normal modes (NNMs) of the physical system depicted in Fig. 1. Moreover, due to the amplitude dependency of the natural angular frequencies, some of the nonlinear mode shapes loose their homogeneity. Some modes can localize when the amplitude increases, i.e. only a small subset of the oscillators are vibrating with significant amplitudes.

The computation of the non-linear modes is carried out by solving Eq.(9) using a continuation procedure. In this study we used the numeric asymptotic method presented in ([34],[35]), and implemented in the MANLAB package. It is common to assume at low amplitude the initial points of the continuation procedure are given by the linear mode shapes, whereas other possible starting points at high amplitude will be described later. The results of the continuation procedure provides the evolution of the natural angular frequency with respect to the amplitude of motion. One also obtains the evolution of mode shapes as the amplitude of vibration increases ([32],[33]). From the results, one can see that some mode shapes are similar (i.e. the shape does not depend on the amplitude of motion), and some others are non-similar. Potential bifurcation points of a given non-linear mode are computed searching for points where the determinant of the Jacobian matrix vanishes. The

Jacobian matrix of Eq. (9) is given by

$$\mathbf{J} = \begin{pmatrix} \xi_1 & -\alpha & 0 & \dots & 0 & -\alpha \\ -\alpha & \xi_2 & -\alpha & 0 & \dots & 0 \\ \dots & & & & & \\ 0 & \dots & 0 & -\alpha & \xi_{N-1} & -\alpha \\ -\alpha & 0 & \dots & 0 & -\alpha & \xi_N \end{pmatrix} \tag{10}$$

with $\xi_n = 1 + 2\alpha - \omega^2 + 9U_n^2$. At high amplitude the nonlinear term will be dominant, hence the linear coupling between the oscillators can be neglected, therefore the system is equivalent to a series of *uncoupled* Duffing oscillators (for $n \in [1, N]$):

$$\ddot{u}_n + u_n + u_n^3 = 0 \tag{11}$$

The eigen-shapes of such a system are given by the vectors of the canonical basis of $\mathbb{R}^N$, and the evolution of the angular frequency (for oscillator n) using a single harmonic HBM is given by $\omega_n^2 = 1 + 3U_n^2$.

In the case of a non-linear modes motion, all (uncoupled) oscillators must have the same frequency, this is possible only if the amplitude are the same for all oscillators ($U_n = U_0$ or $U_n = -U_0$) or if some amplitudes are zero. Therefore, at high amplitude, one expects that the mode shape will have the following general form:

$$\phi_n = u_n, \text{ with } u_n \in \{-1,\ 0,\ 1\} \tag{12}$$

In other words, there are three choices for each component of the mode shape. This leads to 3^{N_s} different mode shapes at high amplitude. Those mode shapes can be used as starting points for relatively high amplitude of motion to initiate the continuation procedure, which is carried out backward, i.e. in the direction of decreasing frequency. However, due to the symmetry of the system, several of those shapes belong to the same "family", i.e. they differ only by a rotation or by a change of sign (see Appendix - A). Without loss of generality, in the following we will choose only one representative for each "family" to drastically decrease the number of possible initial points.

4.2. Nonlinear normal modes analysis for the present system

We start our investigation focusing on periodic solutions from the undamped and unforced nonlinear system (9) assuming $N_s = 6$ and $\alpha = 0.01$.

Therefore, the strategy proposed in Sub. 4.1 is employed to compute the NNMs of the underling conservative regime. The details of the derivation are not reported, while the main results are highlighted here:

- the first NNM $U_n^{k=0}$, when all masses vibrate in phase, is similar (its shape does not change with amplitude) and does not bifurcate;
- the NNM $U_n^{k=1,cos}$ is non-similar and bifurcate twice;
- the NNM starting from $U_n^{k=1,sin}$ is similar and does not bifurcate;
- the NNM starting from $U_n^{k=2,cos}$ is similar and does not bifurcate;
- the NNM starting from $U_n^{k=2,sin}$ is non-similar and bifurcates twice;
- the last NNM $U_n^{k=3}$, when all masses vibrate out of phase, is similar and bifurcates eleven times.

Starting from the linear mode, and following the bifurcations, 22 classes of solutions have been computed (thin solid lines in Fig. 3). From symmetry consideration the number of possible solutions can be reduced from $3^{N_s} = 729$ to 52 (including the trivial solution, see Appendix - A) 22 of which have been computed continuing the linear modes. In order to compute the remaining 30 modes, we use the corresponding shapes as a starting point at high amplitude for the continuation algorithm, and we start the continuation "backward" (i.e. in the direction of decreasing frequency). This allows to compute new branches of solution in the Frequency Energy Plot (FEP) diagram (Fig. 3), where the L^2 norm is defined as

$$L^2 = \sqrt{\sum_{i=1}^{N_s} U_n^2}, \tag{13}$$

The non-linear modes corresponding to those new branches are not connected to the other modes through bifurcation and appear as isolated branches on the FEP diagram (dashed thick red lines in Fig. 3). Those modes do no exist at low amplitude, but appear only after the energy is greater than a given threshold (depending on the mode). At high energy the nonlinear term is dominant and the oscillators behave as isolated. In fact the corresponding NNMs cluster into 6 groups, which energy depends on the number of oscillators vibrating with no negligible amplitude.

Fig. 4 reports some NNMs shapes (we have selected 15 out of the 52 solutions). Notice that possible solutions involve high localized ones with very few oscillators vibrating with appreciable amplitude.

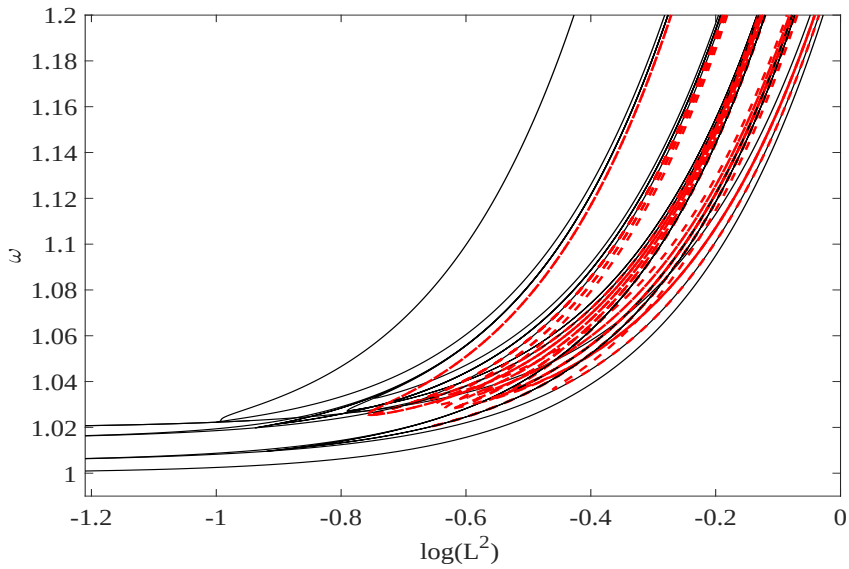

Fig. 3 - FEP diagram of the nonlinear modes with their bifurcation. Thin solid black lines represent the solution of (9) starting, at low energy, from the linear modes. Thick dashed red lines represent the solution of (9) starting at high energy and continuing them towards lower frequency (see Appendix).

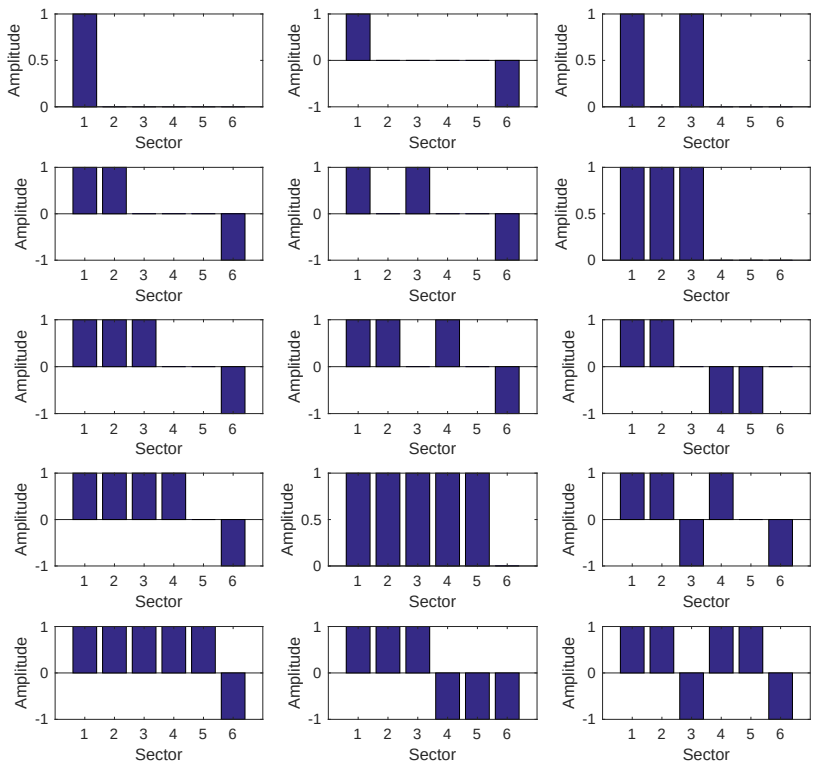

Fig. 4 - A selection of 15 (out of 52) nonlinear normal mode shapes with different degree of localization

5. Nonlinear forced and damped regime

5.1. Solution approach

In the present analysis we investigate the system described by Eq. (3) subjected to an external force

$$g_n(\tau) = \tilde{G}_n \exp\{\mathrm{i}\omega_F \tau\} + \text{c.c.}, \tag{14}$$

where ω_F is the external force angular frequency and $\tilde{G}_n$ is the force amplitude. To find the steady state periodic solutions of the system we adopt the harmonic balance method. Assume that, in the weakly nonlinear regime, the response $u_n(\tau)$ is well approximated by a single harmonic such as

$$u_n(\tau) = \tilde{U}_n \exp\{\mathrm{i}\omega_F \tau\} + \text{c.c.}, \tag{15}$$

where $\tilde{U}_n$ is a constant amplitude. After inserting Eqs. (14) and (15) into Eq. (3) and projecting onto the truncated Fourier basis, the following set of nonlinear algebraic equations is obtained

$$(-\omega_F^2 + 2\mathrm{i}\xi\omega_F + 1 + 2\alpha)\tilde{U}_n - \alpha(\tilde{U}_{n+1} + \tilde{U}_{n-1}) + 3|\tilde{U}_n|^2\tilde{U}_n = G_n \qquad (16)$$

is obtained. Therefore, the amplitudes and phases of $u_n(\tau)$ are defined by the solutions of the algebraic system in Eq. (16).

5.2. Nonlinear forced responses

In this subsection we simulate the system in Fig. 1, as described by the non-dimensional form in Eq. (3), assuming $N_s = 6$ masses, $\xi = 0.005$ and weak coupling condition $\alpha = 0.01$. A harmonic force is applied to each oscillator assuming a constant amplitude and phase value, such as

$$g(\tau) = G_0 \exp\{\mathrm{i}\omega_F\tau\} + \text{c.c.}, \qquad (17)$$

where G_0 is the force amplitude. One should note that the excitation is perfectly orthogonal to all linear normal modes, except the first one which represents vibrations with all masses moving in phase. However, due to the presence of damping, the responses may vibrate with different phase values. For this purpose we used the continuation package AUTO, using as initial conditions highly loacalized guess (e.g. [0,1,0,0,-1,0])

The system frequency response function (L^2-norm vs angular frequency ω_F) is depicted in Fig. 5.

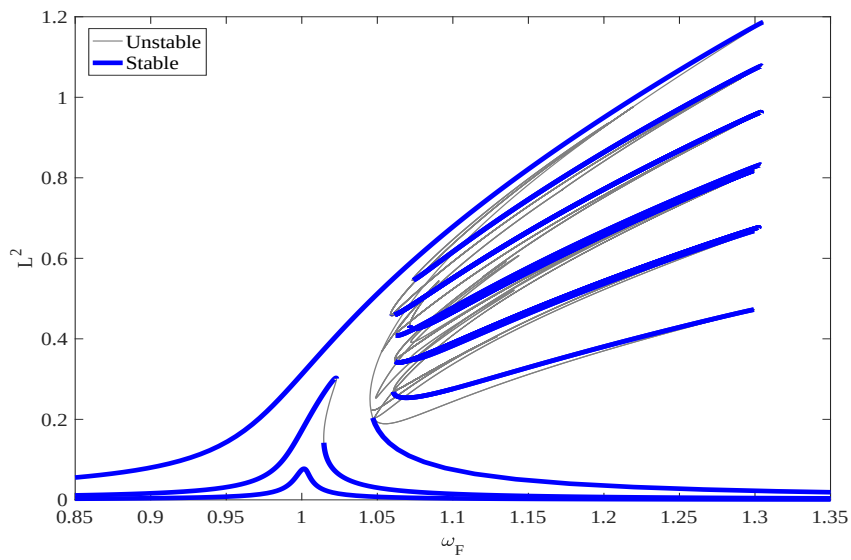

Fig. 5 - Frequency response function obtained for the chain of weakly coupled Duffing oscillators computed for three different force levels $G_0 = [0.32, 1.3, 6.3] \times 10^{-3}$

The results were computed using three different force levels, while blue thick lines indicate linearly stable solutions. The first response, computed for $G_0 = 3.2 \times 10^{-4}$, illustrates the response when the nonlinear force is negligible. The response is linear and single-valued. The second curve, computed for $G_0 = 1.3 \times 10^{-3}$, shows already the stiffening effect induced by the cubic stiffness. However, the responses are still homogeneous and no localization is observed. In the last case, when $G_0 = 6.3 \times 10^{-3}$, the response shows several bifurcated branches. The forced response shows multiple solutions within the frequency interval where the forced single oscillators exhibit two stable solutions for a given exciting frequency. Hence the forced response of the whole system is multivalued with many intertwining branches. The new branches seem to organize themselves similarly to snaking bifurcations ([36–38],[29]). In fact they fold alternating each individual oscillator from an upper branch to a lower one. Therefore, it is possible to observe solutions varying from states where energy is localized in just one oscillator, to solutions when energy is equally spread along the structure. This pattern is not much affected by the particular choice of cyclic (which we are using here) or free-free boundary conditions. Notice that, although the branches seem to

be all connected, in fact they aren't, but appear as isolas of solutions, which get superposed in a two dimensional representation.

In order to provide a closer look at the transition from homogeneous states to localized ones, eq. (3) is solved for four different excitation levels. The results are depicted in Fig. 6 increasing the exciting force from panel (a) to panel (d) respectively. On the left column the frequency response function is reported, while, on the right column, the modulus of the vibration amplitude is shown for the labeled solutions. Linearly stable solutions are drawn with thick blue lines, unstable solutions with thin gray lines. Results in panel (a) have been computed for $G_0 = 1.6 \times 10^{-3}$. It is shown that for low excitation the response is quite homogeneous (Fig. 6, panel (a), right column) and only the unstable solution labeled with "P4" shows some degree of localization. When the force is slightly increased to $G_0 = 2.4 \times 10^{-3}$ (Panel (b)) other branches of solutions are identified. Moreover, spatially localized linearly stable states appear. The bifurcation picture is mainly composed of two localized states detaching from the homogeneous solutions (P1 and P2), and two isolas that do not bifurcate from the main solution (solutions P3 and P4). Panel (c) and (d) are computed for $G_0 = 3.2 \times 10^{-3}$ and $G_0 = 6.4 \times 10^{-3}$ respectively. It is shown that increasing the external excitation more branches are identified, and the isolas seem to evolve towards a final states where they merge with the upper branch of localized solution. Finally the final "snaking bifurcation pattern" appears where the vibration gets localized from one single oscillator to the final homogeneous configuration either in the upper or in the lower branches. Comparing Fig. 4 and Fig. 6 one also notice the similarities between the NNM and forced responses shapes. Indeed, this behavior should be expected, as it is well known that the NNMs are the "backbone curves" of the forced response and, at the resonance point, the forced system behaves alike the underlying NNM.

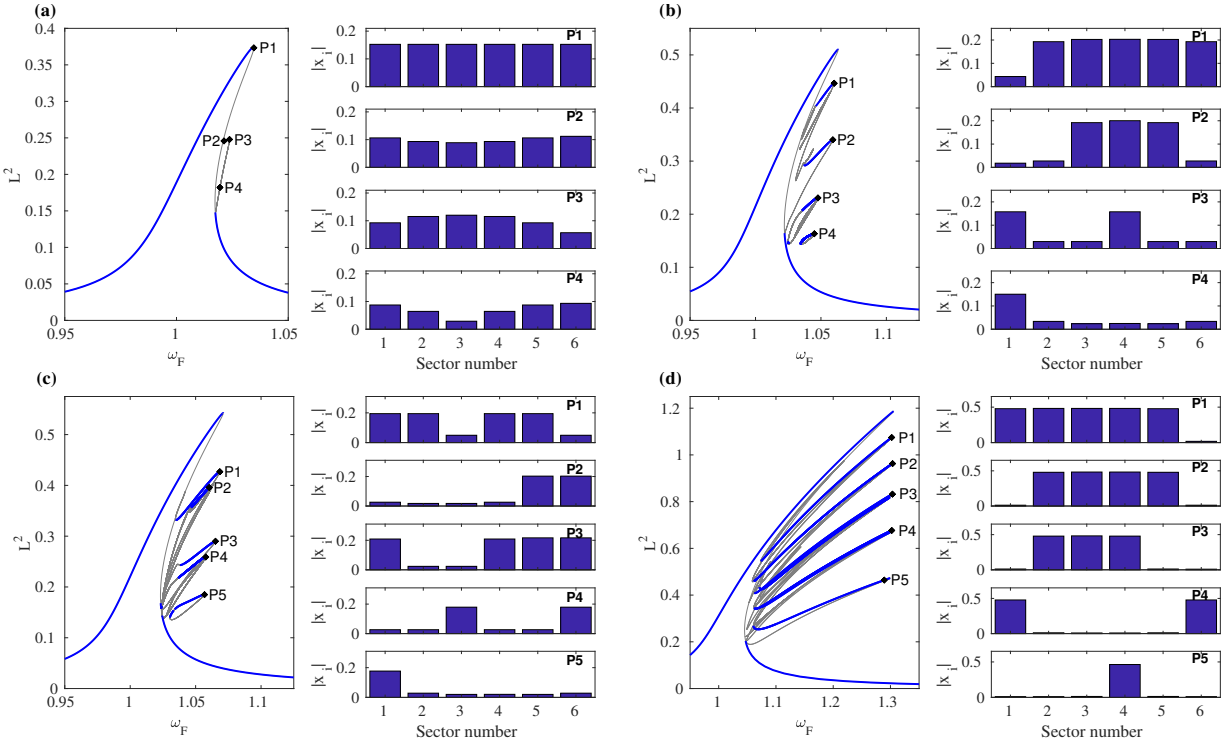

Fig. 6 - Form panel (a) to panel (d) the excitation force is $G_0 = [1.6, 2.4, 3.2, 6.4] \times 10^-3$ respectively. For each panel on the left column: frequency response function (blue thick lines for linearly stable solutions, thin gray lines for unstable solutions). For each panel on the right column: vibration amplitude (in modulus) for each sector

In Fig. 7 the nonlinear normal modes of the dynamical system (thin dashed lines) are superposed on the forced response (only stable solutions are reported with thick solid lines) for $G_0 = 6.3 \times 10^{-3}$. It is clearly shown that the local resonances of the mechanical systems are associated to a particular backbone curve. At high energy the response clearly clusters into 6 groups which correspond to the number of oscillators involved in the vibration.

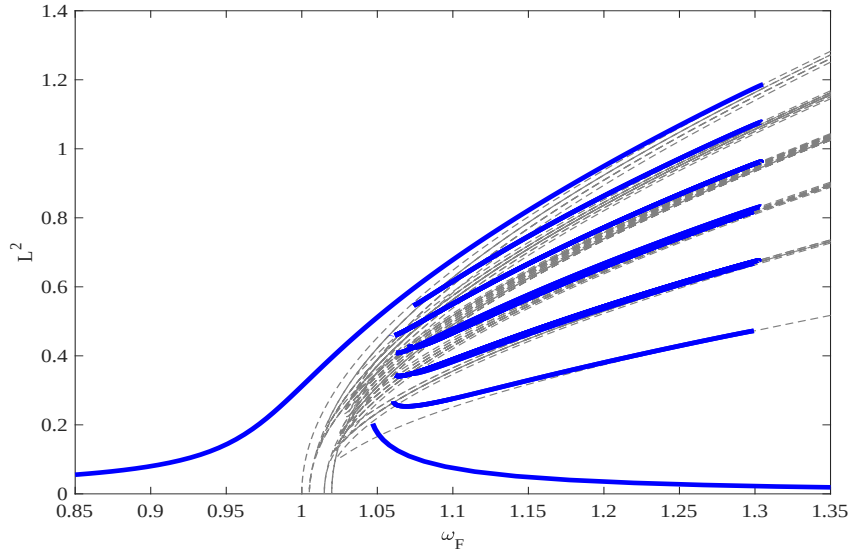

Fig. 7 - The frequency response function of the mechanical system for $G_0 = 6.3 \times 10^{-3}$ is superposed to the NNMs. Only the stable solutions of the forced response are reported, while dashed lines represent the NNMs.

6. Conclusions

In this paper, the problem of vibration localization in externally excited weakly-coupled cyclic symmetric structures affected by geometrical nonlinearities has been considered. The model we have set-up is constituted by a cyclic symmetric chain of six Duffing oscillators, where stiffening effects have been considered via a cubic stiffness term. The nonlinear normal modes have been computed. Due to symmetry considerations, the system periodic solutions can be classified into 52 different shapes (including the trivial one). It has been shown that 22 of them are obtained starting from the linear modes and following their bifurcation from low to high amplitude. The remaining 30 solutions, instead, appear to be isolated branches, detached from the other modes. The isolated branches exist only after a certain energy threshold is reached and disappear at low energy.

When the cyclic symmetric chain is forced with the first linear mode shape (all the oscillators are excited with the same force) spatial localized vibrating states appear. The degree of localization is strongly dependent on the excitation strength. For strong excitation more localized branches

appear, which, in the bifurcation diagram arrange similarly to snaking bifurcations. When the backbone curves of the nonlinear normal modes are superposed with the forced response they appear to match almost exactly, showing that the intermediate states between the low and high energy states correspond to local resonances of the system. We have shown that this behaviour is strongly related to the bistable behaviour of the single nonlinear oscillators from which the chain is formed: if the excitation level is low, the bistable range disappears, the system behaves nearly linearly and there is no localization. In the latter case, there is no localization.

The results of the present study may be of interest for aerospace/aeronautical applications, where the quest of high performance is leading to lightweight and slender structures, often characterized by weak nearest neighbor coupling (e.g. fan blades or antennas). Due to high flexibility, the latter are prone to large oscillations thus to nonlinear stiffening effects. This work shows that vibration spatial localization can arise due to nonlinear phenomena, which represents a different mechanism with respect to mistuning. Further studies are needed to better understand how the presently demonstrated nonlinearly triggered localization effect interacts with linear localization phenomena such us mistuning.

Author Contribution Statement

AP and FF conceived the work. FF computed the numerical results. AG did the NNM analysis. AP wrote the paper and coordinated all the work. MC and NH supervised the work.

Acknowledgements

AP is thankful to the DFG (German Research Foundation) for funding the projects PA 3303/1-1 and HO 3852/11-1.

Appendix A: sorting initial points using symmetry

Denote E the set of all possible initial points at high amplitude. There are $|E| = \text{card}(E) = 3^{N_s}$ possible choices, i.e. 3 choices $[1, 0, -1]$ for the N_s components.

In order to reduce the number of initial points, one can use the fact that the algebraic system defining the non-linear modes in Eq. (9) is equivariant under several groups:

- The cyclic group $\mathcal{C}_N$, which representation in a N dimensional space is generated by the $N \times N$ matrix $\mathbf{R}$ given by the following:

$$\mathbf{R} = \begin{pmatrix} 0 & 1 & 0 & 0 & 0 & 0 \\ 0 & 0 & 1 & 0 & 0 & 0 \\ \vdots & & & \ddots & & \vdots \\ 0 & 0 & 0 & 0 & 1 & 0 \\ 0 & 0 & 0 & 0 & 0 & 1 \\ 1 & 0 & 0 & 0 & 0 & 0 \\ & & & & & \end{pmatrix} \tag{18}$$

- The axial symmetry, generated by the $N \times N$ matrix $\mathbf{S}$ given as:

$$\mathbf{S} = \begin{pmatrix} 1 & 0 & 0 & 0 & 0 & 0 \\ 0 & 0 & 0 & 0 & 0 & 1 \\ 0 & 0 & 0 & 0 & 1 & 0 \\ \vdots & & & \iddots & & \vdots \\ 0 & 0 & 1 & 0 & 0 & 0 \\ 0 & 1 & 0 & 0 & 0 & 0 \\ & & & & & \end{pmatrix} \tag{19}$$

- The "sign-change" symmetry (related to the fact that we are looking for "symmetric" periodic solution such that $u(t + \frac{T}{2}) = -u(t)$), generated by the $N \times N$ matrix $\mathbf{C}$ given as:

$$\mathbf{C} = \begin{pmatrix} -1 & 0 & 0 & 0 & 0 \\ 0 & -1 & 0 & 0 & 0 \\ \vdots & & \ddots & & \vdots \\ 0 & 0 & 0 & -1 & 0 \\ 0 & 0 & 0 & 0 & -1 \\ & & & & \end{pmatrix} \tag{20}$$

To sum up the algebraic system is equivariant under a group G, having $|G| = 4N$ elements, which can be represented as:

$$G = \{g_{ijk} = \mathbf{S}^i \mathbf{C}^j \mathbf{R}^k, \text{ with } (i,\ j,\ k) \in [0,\ 1] \times [0,\ 1] \times [0,\ N-1]\} \tag{21}$$

For the case $N_s = 6$ taking into account the symmetry conditions, the number of initial points reduces from $|E| = 3^{N_s} = 729$ to only 52, which includes the trivial one with all 0.

References

References

[1] R. Bartels, A. Sayma, Computational aeroelastic modelling of airframes and turbomachinery: progress and challenges, Philos. Trans. R. Soc. A 365 (1859) (2007) 2469e2499, https://doi.org/10.1098/rsta.2007.2018

[2] D. J. Ewins, The effects of detuning upon the forced vibrations of bladed disks. Journal of Sound and Vibration, 9(1) (1969) 65IN273-7279.

[3] A. Martin, F. Thouverez, Dynamic Analysis and Reduction of a Cyclic Symmetric System Subjected to Geometric Nonlinearities. ASME. Turbo Expo: Power for Land, Sea, and Air, Volume 7C: Structures and Dynamics ():V07CT35A015. doi:10.1115/GT2018-75709.

[4] O.O. Bendiksen, Mode localization phenomena in large space structures, AIAA Journal, Vol. 25, No. 9 (1987), pp. 1241-1248.

[5] A. J. Dick, B. Balachandran, & C. D. Mote, Intrinsic localized modes in microresonator arrays and their relationship to nonlinear vibration modes, Nonlinear Dynamics, 54.1-2, (2008), 13-29.

[6] A. J. Dick, B. Balachandran, & C.D. Mote, Localization in microresonator arrays: influence of natural frequency tuning. Journal of Computational and Nonlinear Dynamics, 5(1), (2010), 011002.

[7] C. H. Hodges, Confinement of vibration by structural irregularity. Journal of sound and vibration, 82(3) (1982) 411-424.

[8] D. S. Whitehead, (1966). Effect of mistuning on the vibration of turbomachine blades induced by wakes. Journal of Mechanical Engineering Science, 8(1), 15-21.

[9] M.P. Castanier, P. Christophe, Modeling and analysis of mistuned bladed disk vibration: current status and emerging directions. Journal of Propulsion and Power 2 (2006) 384-396

[10] P.W. Anderson, Absence of diffusion in certain random lattices, Phys. Rev., 109(5) (1958) 1492-1505.

[11] K.Y. Sanliturk, D. J. Ewins, A. B. Stanbridge. Underplatform dampers for turbine blades: theoretical modelling, analysis and comparison with experimental data. ASME 1999 international gas turbine and aeroengine congress and exhibition. American Society of Mechanical Engineers, 1999.

[12] C. M. Firrone, S. Zucca,. Underplatform dampers for turbine blades: The effect of damper static balance on the blade dynamics. Mechanics Research Communications, 36(4) (2009) 515-522.

[13] A. Papangelo, M. Ciavarella, On the limits of quasi-static analysis for a simple Coulomb frictional oscillator in response to harmonic loads. Journal of Sound and Vibration, 339, (2015) 280-289.

[14] A. Papangelo, M. Ciavarella. Optimal normal load variation in wedge-shaped Coulomb dampers. The Journal of Strain Analysis for Engineering Design, 51(4), (2016) 279-285.

[15] L. Pesaresi, L. Salles, A. Jones, J.S. Green, C.W. Schwingshackl. Modelling the nonlinear behaviour of an underplatform damper test rig for turbine applications. Mechanical Systems and Signal Processing, 85, (2017) 662-679.

[16] L. Pesaresi, L. Salles, R. Elliott, A. Jones, J. S. Green, C. W. Schwingshackl. Numerical and experimental investigation of an underplatform damper test rig. In Applied Mechanics and Materials (849), (2016) 1-12

[17] A.F. Vakakis, L.I. Manevitch, Y.V. Mikhlin, V.N. Pilipchuk, A.A. Zevin, Normal Modes and Localization in Nonlinear Systems, John Wiley & Sons Inc, New York, 1996.

[18] G. Kerschen, M. Peeters, J.C. Golinval, A.F. Vakakis, Nonlinear normal modes, Part I: a useful framework for the structural dynamicist, Mech. Syst. Signal Process. 23 (1) (2009) 170e194, https://doi.org/10.1016/j.ymssp.2008.04.002.

[19] A. Papangelo, A. Grolet, L. Salles, N. Hoffmann, M. Ciavarella, Snaking bifurcations in a self-excited oscillator chain with cyclic symmetry. Communications in Nonlinear Science and Numerical Simulation, 44 (2017a) 108-119.

[20] A. Papangelo, M. Ciavarella, N. Hoffmann, Subcritical bifurcation in a self-excited single-degree-of-freedom system with velocity weakening-strengthening friction law: analytical results and comparison with experiments. Nonlinear Dynamics, 90(3) (2017b) 2037-2046.

[21] A. Papangelo, N. Hoffmann, A. Grolet, M. Stender, M. Ciavarella, M., Multiple spatially localized dynamical states in friction-excited oscillator chains. Journal of Sound and Vibration, 417 (2018) 56-64.

[22] A. Grolet, F. Thouverez, Free and forced vibration analysis of a nonlinear system with cyclic symmetry: Application to a simplified model. Journal of sound and vibration, 331(12) (2012) 2911-2928.

[23] F. Fontanela, A. Grolet, L. Salles, A. Chabchoub, N. Hoffmann, Dark solitons, modulation instability and breathers in a chain of weakly nonlinear oscillators with cyclic symmetry, Journal of Sound and Vibration, 413 (2018) 467-481.

[24] Y. Starosvetsky, L.I. Manevitch, On intense energy exchange and localization in periodic FPU dimer chains, Phys. D: Nonlinear Phenom. 264 (2013) 66-79, https://doi.org/10.1016/j.physd.2013.06.012.

[25] M.P. Castanier, C. Pierre, Using intentional mistuning in the design of turbomachinery rotors, AIAA J. 40 (10) (2002) 2077e2086, https://doi.org/10.2514/3.15298.

[26] F. Georgiades, M. Peeters, G. Kerschen, J.C. Golinval, M. Ruzzene, Modal analysis of a nonlinear periodic structure with cyclic symmetry, AIAA J. 47 (4)(2009) 1014e1025, https://doi.org/10.2514/1.40461.

[27] O.O. Bendiksen, Mode localization phenomena in large space structures, AIAA J. 25 (9) (1987) 1241e1248, https://doi.org/10.2514/3.9773.

[28] O.O. Bendiksen, P.J. Cornwell, Localization of vibrations in large space reflectors, AIAA J. 27 (2) (1989) 219e226, https://doi.org/10.2514/3.10084.

[29] A.R. Champneys, Homoclinic orbits in reversible systems and their applications in mechanics, fluids and optics. Physica D: Nonlinear Phenomena, 112.1 (1998) 158-186.

[30] O. Thual , and S. Fauve, Localized structures generated by subcritical instabilities. Journal de Physique 49.11 (1988) 1829-1833.

[31] C. Beaume, A. Bergeon, E. Knobloch, Homoclinic snaking of localized states in doubly diffusive convection. Physics of Fluids, 23(9) (2011) 094102.

[32] R. M. Rosenberg, The normal modes of nonlinear n-degree-of-freedom systems. Journal of applied Mechanics, 29(1) (1962) 7-14.

[33] S. W. Shaw, C. Pierre, Normal modes for non-linear vibratory systems. Journal of sound and vibration, 164(1) (1993) 85-124.

[34] B. Cochelin, N. Damil and M. Potier-Ferry. " Asymptotic-Numerical Methods and Padé approximants for non- linear elastic structures" Int. J. Numer. Methods Engng , Vol 37, p 1187-1213, 1994.

[35] B. Cochelin. " A path following technique via an Asymptotic-Numerical method" Computers & Structures, Vol 53, $N°$ 5, p 1181-1192, 1994.

[36] Hunt, G. W., Lord, G. J., A.R. Champneys, Homoclinic and heteroclinic orbits underlying the post-buckling of axially-compressed cylindrical shells. Computer methods in applied mechanics and engineering, 170(3-4) (1999) 239-251.

[37] G.W. Hunt, M.A. Peletier, A.R. Champneys, P.D. Woods, M. A. Wadee, C.J. Budd, G.J. Lord, Cellular buckling in long structures. Nonlinear Dynamics, 21(1) (2000) 3-29.

[38] J. Burke, E. Knobloch, Homoclinic snaking: structure and stability. Chaos: An Interdisciplinary Journal of Nonlinear Science, 17(3) (2007) 037102.